First Observation of Orthorhombic Jahn-Teller EPR Spectra in Cu(II) doped $(NH_4)_2Cd_2(SO_4)_3$ (ACS) Single Crystals. Paper I

Dilip K. De[1]
Olin Physical Laboratory, Wake Forest University, Winston-Salem, North Carolina, USA
Department of Physics, Federal University of Technology, Yola, Adamawa State, Nigeria[2]

Since the first experimental confirmation of axial Jahn-Teller effect in Cu(II) doped $ZnSiF_6.6H_2O$ in 1950, the Orthorhombic Jahn-Teller Effect (OJTE) in solids has not been clearly observed experimentally even though a lot of conjectures have been made. This is the first report of experimental observation of orthorhombic Jahn-Teller EPR spectra ^2E Cu(II) ion in cadmium ammonium sulphate crystal providing the direct confirmation of the OJTE. The spectra correspond to all the three Jahn-Teller potential well minima being non-equivalent in energy. The detailed theoretical analysis (not reported here) of the spectra led to evaluation of many spectroscopic parameters and their temperature dependence, suggesting potential applications of such systems.

1. Introduction

In 1956 Jona and Pepinsky [1] discovered the langbeinite family of crystals with a general formula $(A^+)_2(B^{2+})_2(SO_4)_3$, where A^+ is ammonium or a monovalent metal ion and B^{2+} a divalent metal ion. These crystals are in general ferroelectric [2] and their structural phase transitions have been the subject of a number of investigations in the past [3]. A number of investigations on the microscopic properties of the langbeinite family of crystals by different researchers have been summarized by Babu et al. [3]. The compound ammonium cadmium sulphate, $(NH_4)_2Cd_2(SO_4)_3$ abbreviated as (ACS), which is of primary interest in this present study, is isomorphous to potassium magnesium sulphate, $K_2Mg_2(SO_4)_3$ and both of them belong to the langbeinite family of crystals [1]. The detailed x-ray data regarding the atomic positions in ACS does not seem to be available in the literature but that of $K_2Mg_2(SO_4)_3$ has been reported by Zemann and Zemann [4]. Tatsuzaki [5] and Hikita et al. [6, 7], have shown that the langbeinite family crystallizes in cubic space group $P_{2/3}$ with a = 10.35 A with four molecules per unit cell. The structure consists of a group of $(SO_4)^{2-}$ tetrahedron, $(NH_4)^{2+}$ tetrahedral and Cd^{2+} metal ions. The NH_4^+ and Cd^{2+} ions lie on the three fold axes and the SO_4^{2-} are in general position. There are two crystallographically non-equivalent sites for each of the Cd^{2+} and $(NH_4)^+$ ions. Every Cd^{2+} is surrounded by six oxygen atoms which form a slightly distorted octahedron. The dielectric measurements carried out by Jona and Pepinsky [1] and Raman spectroscopy by Rabkin et al. [8] have yielded substantial information on the structural phase transition (SPT) in ACS. They observed that ACS exhibits a SPT on lowering the temperature from space group $P_{2/3}$ to P_{21} at about 95 K, the lower temperature phase being ferroelectric.

Spectroscopy has been used to study the microscopic mechanism responsible for phase transition in ACS. EPR studies [5, 9] of ACS appear to suggest the freezing of SO_4^{2-} rotations, along with NH^{4+} rotations, in the vicinity of the phase transition at 95 K (-178 ^oC) ($P2_13$ P21), presumably due to onset of hydrogen bonding between the H^+ in NH^{4+} and the oxygen in the SO_4^{2-} ion. Misra and Korezak's EPR [10] study using Mn^{2+} as the probe ion revealed a phase transition at 94.5 $\pm$ 0.5 K; they confirmed the freezing out of the rotation of the $(SO_4)^{2-}$ ion at phase transition, as predicted earlier [5, 9]. They observed four sets of 30 lines Mn^{2+} spectra in the [111] plane corresponding to four magnetically nonequivalent ions in a unit cell.

Also Mouli and Sastry [11] study of the EPR spectra of Cu^{2+} doped ACS at room temperature and 77 K yielded eight poorly resolved hyperfine lines in a general direction and a set of four unresolved hyperfine lines in any crystallographic plane corresponding to two nonequivalent ions in a unit cell. Their computed g-values showed that $g_{//}>g_{\perp}$ and that the A_{max} is falling along g_{min}. They concluded that Cu^{2+} ions in this crystal may be in a compressed octahedral position or enter interstitially rather than substitutionally. The shortcomings of the study of Mouli and Sastry include its limitation to 77 K and its failure to focus on JT effect that could be associated with Cu^{2+} in

[1] dipak61@yahoo.com
[2] Present address.

this crystal as hinted later by Babu et al. [3]. Bhat et al.'s [5] EPR spectra of Mn^{2+} ion in two phases $P_{2/3}$ and P_{21} of ACS at room temperature and at 77 K were slightly different, particularly in the magnitudes of their zero- field splitting, as a result of small orthorhombic component in the low temperature phase [3]. The differences in the spectra indicated a phase transition from higher temperature phase $P_{2/3}$ to a low temperature phase (probably) of $P_{2/1}$. In 1975 Ng and Calvo [12] studied EPR spectra of Mn^{2+} in ACS in the range 300 K to 77 K. Their study revealed a definite change of spectral pattern from that of room temperature to that of liquid Nitrogen temperature due to a phase transition from $P_{2/3}$ to a space group of lower symmetry at low temperature. They did not analyze the spectra nor determine the phase transition temperature due to the complexity of the spectra at liquid nitrogen temperature.

Babu et al. [3] (1984) study of phase transition in ACS using VO^{-2} as a probe in the temperature range of 573-77 K obtained a complex spectrum in which they were unable to identify the phase transition temperature and suggested that the lower temperature phase stabilizes at temperatures higher than 95 K. This was due to a local stabilization of the low symmetry phase by vanadyl ions. They also found that the data of their experiment contained Cu^{2+} ion as contaminant and thus concluded that the complication in their results could have been due to a possible JT effect associated with Cu^{2+} ion in this crystal. Unfortunately, they did not carry out further investigation to establish or rule out the possibility of JT effect due to Cu^{2+} ion in this crystal.

In order to resolve the question of Jahn-Teller effect of Cu^{2+} in ACS we have carried out detailed EPR study of Cu^{2+} doped in ACS at various temperatures in the range 300 – 15 K with angular variations usually at steps of 5^o and 0.5^o near Jahn-Teller extrema points in three mutually perpendicular planes of ACS single crystal. We find that Cu^{2+} ion in ACS exhibits static Jahn-Teller effect and for the first time we report the observation of simultaneous appearance of orthorhombic EPR Jahn-Teller spectra from a ^2D ion (with ^2E ground state) in this system at 15 K. Detailed theoretical studies of this interesting observation would follow this paper separately.

2. Experimental Details

Single crystals of CAS were grown by evaporation at controlled temperature 358 K, from an aqueous solution containing stoichiometric amounts of $CdSO_4{,}8H_2O$ and $(NH_4)_2SO_4$, to which was added an appropriate amount of $CuSO_4$, such that there is one Cu^{2+} ion for every 100 Cd^{2+} ions in the solution. In about one month's time optically clear single crystals devoid of any twinning were obtained.

The EPR spectra were performed with a Varian E-century line spectrometer operating at 9.28 GHz. An APD cryogenics HC-4 closed cycle refrigerator was used to vary the temperature of the sample in the EPR cavity in the temperature range 15 – 300 K. The spectra were recorded in three mutually perpendicular planes of crystals viz: ab, ac and bc planes with angular variations of usually 5^o and $\pm 0.5^o$ in the neighborhood of the locations of the extrema points of the Jahn-Teller EPR spectra. While measuring the g and A as reported in Table 1, proton NMR was used to measure the magnetic fields accurately (not shown in Fig. 1).

3. Results and Discussion

In the ac plane of the crystal, the spectra consist of four poorly resolved isotropic hyperfine lines at room temperature 300 K and above. The resolution improved significantly as the temperature is lowered. This is primarily due to reduction in broadening as a result of reduction in spin-lattice relaxation rate at lower temperatures. At the lowest temperature of 15 K (attainable in our experiment), we have performed EPR spectra with angular variations in all three planes ab, ac and bc. In ac plane at certain orientation say X, the spectra at 15 K consists of a set of very well resolved four hyperfine lines (from Cu^{2+}, nuclear spin I =3/2) at the lowest field (corresponding to g_z and A_z) and two sets of four well resolved hyperfine lines at the highest fields (corresponding to g_x, g_y and A_x, A_y). g_x, g_y, g_z and A_x, A_y and A_z are the components (principle axes) of the g and A tensors of Cu^{2+} ion. Fig. 1 shows the temperature evolution of the EPR spectra in ac plane of the crystal along a direction, say X, that gives the largest separation between the group of low and high field lines at 15 K. The direction X is not quite along c axis but about 10^o off from c in the ac plane. At this orientation, the hyperfine splitting of the lowest field lines is the highest and that of the highest field lines the lowest. When the crystal is rotated by about 52^o in the ac plane from this direction X, the three sets of four hyperfine lines merge into one set of four hyperfine lines. At any other direction in ac plane, the separation between the low field lines and the high field lines decreases. This and the temperature evolution of the spectra (Fig. 1) remind us the

Table 1: Observed g and A values in Cu(II) doped $(NH_4)_2Cd_2(SO_4)_3$ single crystals measured from the simultaneous Orthorhombic JT EPR spectra in the ac plane of the single crystals at different temperatures along one [100] JT axis.

T±1 K	g_z ±0.005	g_x ±0.005	g_y ±0.005	g_{111} ±0.005	A_z ±2G	A_x ±2G	A_y ±2G	A_{111} ± 2G	I_N ±0.05	ΔH_{pp} ± 2G
15	2.415	2.144	2.094	2.222	104	20	17	62	10.0	12
40	2.412	2.145	2.095	2.221	102	18	14	61	9.0	12
60	2.408	2.146	2.097	2.221	100	18	13	60	6.83	12
80	2.401	2.150	2.101	2.221	96	12	12	56	4.3	12
100	2.393	2.151	2.103	2.219	94				3.63	14
110	2.387	2.153	2.105							
120	2.384	2.155	2.107		91				2.58	16
130	2.376	2.157	2.109							
140	2.370	2.159	2.110		88				1.58	20
150	2.365	2.160	2.111							
160	2.361				84				1.11	22
180	2.353				80				0.76	24
220	2.340				72				0.22	30
240	2.327				72				0.17	33
260	2.322				68				0.08	33

possibility of Jahn-Teller effect due to Cu^{2+} ion in this crystalline ACS. The direction X may be identified as one of the [100] axes of the Cu^{2+} ion complex. Let us consider a system where Cu^{2+} ion exhibits Jahn-Teller (JT) effect with an axially symmetric g and A values. In such a system, there are three JT distortion axes of the type [100], along each of which the EPR spectra would consist of a set of four hyperfine lines occurring at the lowest field (corresponding to the g_{ll} lines) along with a set of four hyperfine lines occurring at the highest field (g lines). In (110) type planes, there is [111] axis at 54.7^o from the [100] axis. Along [111] direction, the two sets of four hyperfine lines merge into one set of hyperfine lines with g and A values satisfying equations (1) and (2) below. This is the signature of static JT effect with a ^2E ion with axial g and A tensors.

$$g_{[111]}^2 = (g_\parallel^2 + 2g_\perp^2)/3 \quad (1)$$

$$A^2_{[111]} = (g_\parallel^2 A_\parallel^2 + 2g_\perp A_\perp^2)/3g_{[111]}^2 \quad (2)$$

The first such EPR spectra was observed by Bleaney and Ingram [13] in $Cu:ZnSiF_6.6H_2O$ crystals that led to the experimental confirmation of Jahn-Teller effect [14] in a ^2E ground state ion with axial g and A tensor. Jahn-Teller distortions in such a system may be classified as axial Jahn-Teller distortion. Later, EPR static JT spectra from a ^2D ion (^2E ground state) with axially symmetric g and A tensors have been observed to satisfy Eqns. 1 and 2 in other systems [15, 16].

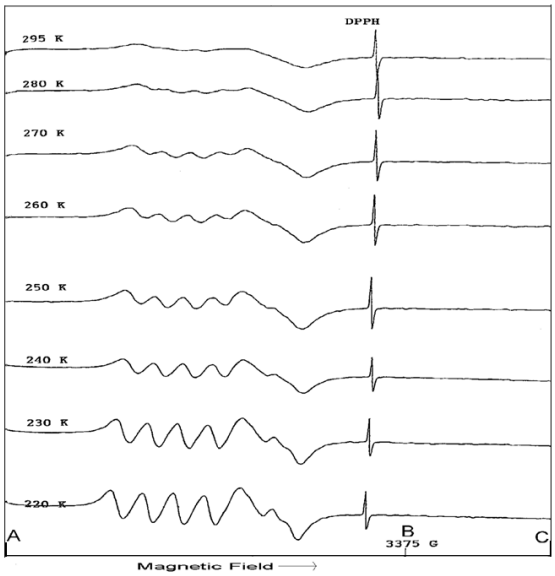

Fig. 1a: EPR spectra of Cu(II) doped $(NH_4)_2Cd_2(SO_4)_3$ (ACS) Single Crystals in AC plane along [100] JT axis at 9.24 GHz in the temperature range 295 K to 200 K. The magnetic field values at A, B and C are 0.2450, 0.3375 and 0.3720 Tesla respectively.

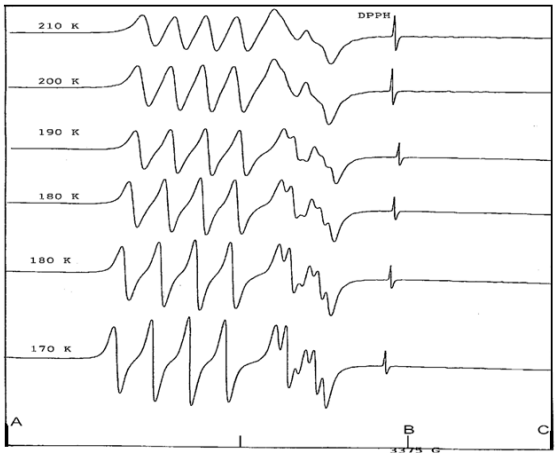

Fig. 1b: EPR spectra of Cu(II) doped $(NH_4)_2Cd_2(SO_4)_3$ (ACS) Single Crystals in AC plane along [100] JT axis in the temperature range 210-170 K at 9.29 GHz. The magnetic field values at A, B and C are 0.2425, 0.3375 and 0.3700 Tesla respectively.

In the case of EPR spectra from a ^2E ground state ion with orthorhombic Jahn-Teller distortions, g and A tensors will also be orthorhombic and Eqns. 1 and 2 are modified to

$$g_{[111]]}^2 = (g_z^2 + g_x^2 + g_y^2)/3 \quad (3)$$

$$A^2_{[111]} = (g_z^2 A_z^2 + g_x^2 A_x^2 + g_y^2 A_y^2)/3g_{[111]]}^2 \quad (4)$$

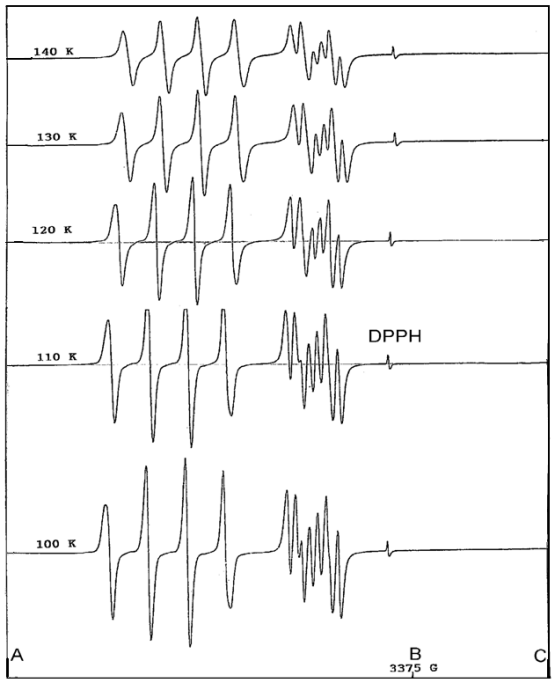

Fig. 1c: EPR spectra of Cu(II) doped $(NH_4)_2Cd_2(SO_4)_3$ (ACS) Single Crystals in AC plane along [100] JT axis at 9.30 GHz in the temperature range 100-140 K. The magnetic field values at A, B and C are 0.2400, 0.3375 and 0.3700 Tesla respectively.

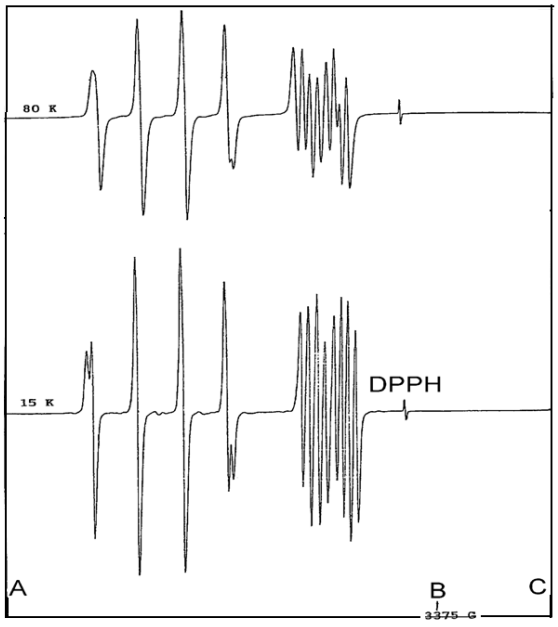

Fig. 1d: EPR spectra of Cu(II) doped $(NH_4)_2Cd_2(SO_4)_3$ (ACS) Single Crystals in AC plane along [100] JT axis at 9.28 GHz at 15 K and 80 K. The magnetic field values at A, B and C are 0.2375, 0.3375 and 0.3650 Tesla respectively.

The spectra along the X direction at 15 K, is of prime interest too us. The orthorhombic JT EPR spectra (Fig. 1) reminds us the multiple EPR lines obtained in the case of the static JT systems Cu(II):$ZnTiF_6.6H_2O$ [15] and Cu(II):$MgSiF_6.6H_2O$ [16]. In the latter cases, the EPR spectra were interpreted as arising from the axial Jahn-Teller distortions of two non-equivalent Cu(II) ions per unit cell. The principal g and A values observed in the static regime are the same for each ion. However, in the present case, we believe that the EPR spectra (Fig. 1) corresponds to orthorhombic static Jahn-Teller effect from one Cu(II) ion per unit cell in ACS crystal for the following reasons:

1. Let us assume that the spectra (Fig. 1a-d) arises from more than one Cu(II) ion per unit cell in ACS. If we assume no Jahn-Teller effect being manifested in this crystal with Cu(II) ion, then there have to be three magnetically non-equivalent ions in ACS so as to give rise to the spectra seen at 15 K (Fig. 1d). In such cases, it is very unlikely that the low field extrema (corresponding to g_{ll} lines) will occur simultaneously with the highest field lines ($g_\perp$). Moreover, they would not merge into one set of four hyperfine lines at angle ~52^o from that of the orientation X, where the three sets of four hyperfine lines at extreme magnetic field values are seen at 15 K(Fig. 1d).
2. Let us assume that there exist two or more Jahn-Teller, active but non-equivalent, Cu(II) ions with axial g and A tensor per unit cell in ACS as in Cu(II):$ZnTiF_6.6H_2O$ [15]. In such a case along the (100) direction, since each ion would give rise to two sets of hyperfine lines at extreme g values contrary to present observations, we would have seen contrary to the observation, more than three sets of four hyperfine lines in at least one of the three planes ab, ac and bc.
3. If there is only one Jahn-Teller active ion per unit cell of ACS with axial g and A tensor, then there is no way we will observe three sets of four hyperfine lines simultaneously occurring along one [100] JT axis. We would observe only two sets of hyperfine lines ($g_\parallel$ and $g_\perp$) similar to the case of Cu:$ZnSiF_6.6H_2O$ [13].
4. The only possible explanation of our present observation (Fig. 1) is that the EPR spectra (Fig. 1) corresponds to one JT Cu(II) ion per unit cell with orthorhombic JT distortions leading to orthorhombic g and A tensor. Further confirmation comes from the measured g and A values along the direction 52^o from that of Fig.1. In that direction, which may be identified as one of the [111] axes of the complex, as said earlier, all the sets merge into a set of four hyperfine lines where the measured g value (2.222) and A value (64 G) agree with the Eqns. 3 and 4 (Table 1). Moreover, the EPR spectra at room temperature are isotropic in all the three planes. They become anisotropic with increasing anisotropy in g and A values as the temperature is lowered and maximum anisotropy is seen at the lowest temperature (15 K) available for the experiment.

The splitting of the $m_I = \pm 3/2$ hyperfine transitions at the $\mathbf{g}_\parallel$ lines is due to the ^{65}Cu ion (I=5/2). The normalized average intensity (I_N) of the lowest field hyperfine lines(g_z) have also been measured as a function of temperature and are given in Table 1 (where $I_N = I_{sample}/I_{DPPH}$). It can be seen from the Table 1 that the line width decreases with temperature. This is believed to be caused by spin-lattice relaxation time ($1/T_1$), which is strongly temperature dependent for Jahn-Teller ions, and decreases with the lowering of temperature.

The manifestation of the Jahn-Teller effect of a ^{2}E ground state ion with orthorhombic g and A tensors as seen in the present case requires the three JT potential wells to be all energetically non-equivalent, meaning that their minima occur at different energies. Challis et al. [17] observed resonant phonon scattering at 300 GHz in $Ni^{2+}(^3T_1)$: GaAs system and attributed the resonant scattering to tunneling within the (ground) states resulting from orthorhombic Jahn-Teller distortions of the system due to coupling between orbital states and phonons arising out of strong e-ph interactions. Parket et al. [18] discussed the possibility of orthorhombic JT effect in the explanation of the EPR spectra in Cr^{3+} in GaAs. They claimed to have observed orthorhombic Jahn-Teller effect in the system from the first excited state ^{2}E of Cr^{3+} ion lying closely above the $^4T_1$ ground state in GaAs. The strong e-ph coupling giving rise to the effect is probably due to certain random strains (that can vary from tetragonal to orthorhombic), which plays an important role in determining the experimental results in the Cr^{3+}:GaAs system. Orthorhombic g values have been derived by Massa et al. [19] from the Cu(II) EPR spectra in the dynamic Jahn-Teller system copper(II) doped Diaquee (L-aspartato) Zn(II) hydrate. Hitchman et al. [20] also derived orthorhombic g values from the dynamic JT EPR spectra of two copper complexes. Misra and Wang reported extraction of orthorhombic g values in Cu(II): Cu:$Cd(NH_4)_2(SO_4)_2.6H_2O$ [21] crystals and

explained their temperature variation with pseudo-Jahn-Teller effect. Orthorhombic JT(OJT) effect is conjectured by Pinsard et al. [22] to be playing an important role in $La_{0.875}Sr_{0.125}MnO_3$ undergoing successive structural phase transitions in the range 400 – 100 K. The effect [23] influences the variations in crystal structure and magneto-resistance in the $La_{1-x}Li_xMnO_3$ (x = 0.10, 0.15, 0.20, 0.30). Bersuker [24] discussed the OJT effect observed in some Cu(II) doped crystals. In $TbVO_4$ crystals, the JT effect is shown [25] to cause magnetic field dependent transition from tetragonal to orthorhombic phase below 33 K. The JT effect [26] is reported to cause large variations (orthorhombic distortions) in the three Mn-O bond lengths and angles in $La_{7/8}Sr_{1/8}Mn_{1-r}O_{3+\delta}$ compounds in the temperature range 298-180K. The orthorhombic structure of the giant magneto-resistance perovskite $LaMnO_3$ appears to be characterized by an antiferrodistortive orbital ordering due to Jahn-Teller effect [27]. None of the above works showed completely resolved orthorhombic JT EPR spectra and their temperature variations as obtained in the present system of Cu(II):ACS. We believe that this is the first report of a clear and direct observation of a static orthorhombic JT EPR spectra with a Cu(II) ion in ^2E ground state at 15 K.

If the magnetic field is oriented along z-direction (100) direction of one of the orthorhombic JT distortions of the Cu(II) ion in ACS, the field H_Z sees the g_z as well g_x, g_y tensor axes simultaneously unlike non-JT ions, and the Spin Hamiltonian H_s becomes, for H along z, i.e., $H_x = H_{y.} = 0$

$$H_S = \beta\left(H_z S_z g_z + H_z S_x g_x + H_z S_y g_y\right) + A_z\left(S_z I_z + S_x I_x + S_y I_y\right) + A_x(2S_x I_x + S_z I_z) + A_y\left(2S_y I_y + S_y I_y\right) \quad (5)$$

Considering the hyperfine interactions as perturbations up to second-order instead of a single transition between the non-JT Kramer's doublet, we have three transitions for H // z direction (in the case of a single Cu^{2+} ion per unit cell in the static JT regime) for JT Kramer's doublet as follows (assuming that the principal axis of the g-tensor ellipsoid coincides, in orientation, with the principal axes of the hyperfine terms):

$$h\nu = g_z\beta H_{zz} + A_z M_I + \frac{(A_x^2 + A_y^2)}{4g_z\beta H_{zz}}\left(I(I+1) - M_I^2\right)) \quad (6)$$

$$h\nu = g_x\beta H_{zx} + A_x M_I + \frac{A_z^2}{2g_x\beta H_{zx}}\left(I(I+1) - M_I^2\right) \quad (7)$$

$$h\nu = g_y\beta H_{zy} + A_y M_I + \frac{A_z^2}{2g_y\beta H_{zy}}\left(I(I+1) - M_I^2\right) \quad (8)$$

For magnetic field parallel to the z axis, the EPR transitions occur at different values of H_{zz}, H_{zx} and $H_{zy,}$ corresponding to the JT ions with their $g_{z,}$ g_x, g_y distortion axes parallel to the magnetic field (along z). This feature is strikingly unique and different from that of a non-JT paramagnetic ion and that of a Jahn-Teller ^2E ion with axially symmetric g and A tensor. Eqns. 6-8 form the basis of derivations of the EPR line shapes equation for the present system. The detailed theory of this effect and analysis of the observed temperature dependences of the orthorhombic EPR Jahn-Teller spectra (Fig. 1) led to evaluation of many spectroscopic parameters and their temperature dependences in Cu(II) doped ACS crystals with effects not seen in this system before and not common with other systems. For example, the energy differences of the three Jahn-Teller potential wells decrease (the difference between two potential wells varies from 25 cm^{-1} at 15 K to 140 cm^{-1} at 150 K) with lowering of temperatures. This is quite in contrast to the temperature dependence seen earlier in JT systems like $Cu(II):ZnTiF_6.6H_2O$[27] , where one JT potential well is lower than the other two (at the same energy). Just before finishing this article, it came to our attention that Misra and Korczac also obtained similar temperature dependences of JT potential energy differences (50 cm^{-1} at 4.2 K to 260 cm^{-1} at 150 K) in Cu(II): $(NH_4)_2Cd(SO_4)_2.6H_2O$ [10], a system different from ours. By looking at the temperature evolution of the single crystal EPR spectra (Fig. 1), one can infer that stabilization of the present system in the JT distorted configuration states occurs at temperatures higher than that observed in earlier systems [14, 15]. The

determination of the energy differences of the three JT potential well minima from observed spectra and the detailed theory confirms this. The cubic to orthorhombic JT transition in Cu(II) doped ACS crystal can be confirmed by performing X-ray structural analysis in doped and un-doped (without Cu(II) ion) crystals at room temperature and low temperature. One interesting question arises. Could the three JT-potential energy levels in such systems be used for lasing actions for values in the neighborhood of 100 cm^{-1} (0.1mm wavelength)? The possible potential applications of such orthorhombic JT systems will be discussed along with the detailed theory of orthorhombic JT EPR spectra and the simulation of the observed spectra reported in Fig.1 in a separate paper following this article.

Acknowledgments

The author gratefully acknowledges the laboratory facilities provided by Prof. Howard Shields, Olin Physical Laboratory, Wake Forest University for the experiments reported here and to Mr. Ferdinand A. Oguama for performing the spectra. The author is grateful to the faculties, specially the chairman Dr. Alex Weiss of the Physics Department, UTA, Arlington, Texas 76019 for providing the facilities and to Narendra N. De for help in preparation of the manuscript.

References

[1] F. Jona and R. Pepinsky Phys. Rev. **103**, 1126 (1956).

[2] R. Vlokh, I. Skab, I. Girnyk, Z. Czapla, S. Dacko and B. Kosturek, Ukranian Journal of Optics **1**(2), 1 (2000).

[3] D. Suresh Babu, G. S. Sastry, M. D. Sastry and A. G. I. Dalvi, J. Phys. C (Solid State Physics) **17**, 4245 (1984) and references therein.

[4] A. Zemann and J. Zemann, Acta Crystallogr. **10**, 409 (1957).

[5] I. Tatsuzaki J. Phys. Soc. Japan **17**, 582 (1312).

[6] T. Hikita, S. Sato, H. Sekiguchi and T. Ikeda, J. Phys. Soc. Japan **42**, 1656 (1977)

[7] T. Hikita, H. Sekiguchi, and T. Ikeda, J. Phys. Soc. Japan **43**, 1327 (1977).

[8] L. M. Rabkin, V. I. Torgashov, L. A. Shuvalov and B. Brezina, Ferroelectrics **36**, 476 (1981).

[9] S. V. Bhat, C. V. Manjunath, R. Kumari Cowsik and R. Srinivasan, Proc. Nuclear Solid State Physics Symp. (Bombay) 1973 Vol.16C, p364.

[10] S. K. Misra and S. Z. Korczak, J. Phys. C: Solid State Phys. **19**, 4353 (1986).

[11] V. C. Mouli and G. S. Sastry, J. Mol. Structure, **96**, 163 (1962).

[12] H. K. Ng and C. Calvo, Can. J. Chem. **53,** 1449 (1975).

[13] B. Bleaney and D. J. E. Ingram, Proc. Roy Soc. A **208**, 143 (1951) and references therein.

[14] H. A. Jahn and E. Teller, Proc. Roy. Soc. A. **161**, 220 (1937).

[15] D. K. De, R. S. Rubins and T. D. Black, Phys. Rev. **29B**, 71 (1984).

[16] R. S. Rubins, L. N. Tello, D. K. De (J) and T. D. Black, J. Chem. Phys. **81**, 4230 (1985).

[17] L. J. Challis, B. Salce, N. Butler, M. S. Tahar and W. Ulrich, J. Phys: Condense Matter **1**, 7277 (1989).

[18] L. W. Parker, C. A. Bates, J. L. Dunn, A. Vasson and A. M. Vasson, J. Phys. Condens. Matter **2,** 2841 (1990).

[19] M. B. Masa, S. D. Dalosto, M. G. Ferreyra, G. Labadie and R. Calvo, J. Phys. Chem. A, **103**, 2606 (1999).

[20] M. A. Hitchman, C. J. Simmons and H. Stratemeier Appl. Mag. Resn. **19**, 121 (2000).

[21] S. K. Misra and C. Wang, Phys. Rev.B. **41**, 1 (1990).

[22] L. Pinsard, J. Rodriguez-Carvajal, A. H. Mondden, A. Anane, A. Revcolevschi and C. Dupas, Physica B (Condensed Matter) **234-236**, 856 (1997).

[23] S. L. Ye, W. H. Song, J. M. Dai, S. G. Wang, K. Y. Wang, C. L. Yuan and Y. P. Sun, J. Appl. Phys. **88**, 5915 (2000).

[24] I. B. Bersuker, in *The Jahn-Teller Effect* (Cambridge, 2006).

[25] C. Detlafs, F. Duc, Z. A. Kazei, J. Vanacken, P. Frings, W. Bras, J. E. Lorenzo, P. C. Canfield and G. L. J. A. Rikken, Phys. Rev. Lett. **100**, 056405 (2008).

[26] H. F. Li, Y. Su, J. Peterson, P. Menffels, J. M. Walter, R. Skowronek and T. H. Brunckel, J. Phys. (Condensed Matter) **19**, 176226 (2007).

[27] J. Rodriguez-Carvajal, M. Hennion, F. Moussa, A. H. Moudden, L. Pinsard and A. Revcolevschi, Phys. Rev. B **57**, R3189 (1998).

[28] Dilip K. De (P) and J. B. Yerima, Int. J. Physical Sciences **3(12)**, 306 (2008).

Received: 6 April, 2010
Accepted: 24 November, 2010